RADIO FREQUENCY INTERFERENCE SUPPRESSION APPLIED TO SYNTHETIC APERTURE RADAR DATA

Richard T. Lord

Radar Remote Sensing Group, Dept. of Electrical Engineering, University of Cape Town
Private Bag, Rondebosch 7701, South Africa
Email: rlord@ebe.uct.ac.za Web: http://www.rrsg.uct.ac.za
Tel: +27 (0)21 650 2792 Fax: +27 (0)21 650 3465

ABSTRACT

This paper addresses techniques of Radio Frequency Interference (RFI) suppression applied to Synthetic Aperture Radar (SAR) data. These techniques could also be used to protect radio-astronomical observations from harmful interference. Of the RFI suppression techniques investigated, the notch filter and the Least Mean Squares (LMS) adaptive filter have been implemented and applied to real P-band data obtained from the E-SAR system of the German Aerospace Center (DLR), Oberpfaffenhofen, and to real VHF-band data obtained from the South African SAR (SASAR) system. Both methods significantly suppressed the RFI in the real images investigated.

INTRODUCTION

RFI is a major problem for low-frequency SAR systems operating in the VHF/UHF-band, because the spectrum is already used extensively by other services such as television, mobile communications, radio and cellular phones. Experience with the South African SAR (SASAR) system [1] has shown that even in remote locations the interference power often exceeds receiver noise by many dB, becoming the limiting factor on system sensitivity and severely degrading the image quality.

RFI is also a major problem for radio astronomy [2, 3], where the influence of RFI ranges from the complete loss of data due to receiver saturation, to very subtle distortions of the data. In radio astronomy, the task of RFI suppression is especially difficult, because the signals of interest, namely the radio frequency emissions from celestial sources, are extremely weak.

APPROACHES TO RFI SUPPRESSION

A number of interference suppression algorithms have been described in the literature [4, 5, 6, 7, 8], many of which require a great amount of computation. Suppressing radio interference from a received signal essentially involves three steps [4]:

1. Finding a model to establish the parameters of the interfering signals;
2. Estimating the parameters of the interfering signals using the measured data;
3. Using the estimated parameters to suppress the interference in the data.

Modelling the interference environment would ideally include information such as the statistics about the density of the interference emitters, the identity (type) of such emitters, and their effective radiated power, modulation bandwidth, duty factor and temporal dependence. The most direct way of achieving this is to make use of "sniffer" pulses or "listening beforehand" schemes [4]. This method is useful for many signal processing methods, but its effectiveness depends significantly on how long the RFI remains coherent. Most approaches model the RFI as a superposition of single sinusoidal "tones", and regard the wideband signal-plus-system noise as white noise. RFI suppression methodologies can be grouped into three main categories [2]:

1. Rejection in the temporal domain (most effective when dealing with strong and spiked bursts of RFI);
2. Rejection in the frequency domain (for weak and long-lasting RFI signals);
3. Spatial filtering (using the difference between the direction-of-arrival of the signal of interest and the RFI).

This paper summarises the work done by the author on RFI suppression algorithms that have been applied to synthetic aperture radar (SAR) data. The notch filter is briefly described, whereas more emphasis has been placed on the LMS adaptive filter, which has been used very successfully to suppress RFI [4, 9, 10, 11].

THE NOTCH FILTER

Since RFI is (usually) narrowband when compared with the transmitted pulse bandwidth, it shows up as narrow spikes in the frequency domain. These spikes are usually many dB stronger than the surrounding signal level. In order to estimate the interference, it is very useful to average a number of magnitude range spectra, because the SAR signal, due to its random nature, will average out, whereas the RFI, due to its often fairly constant nature, will be enhanced. A median filter can be applied to the averaged magnitude spectra, in order to isolate the RFI spikes to be notched out.

THE LMS ADAPTIVE FILTER

Fig. 1 shows a schematic of the LMS adaptive filter as it is used for RFI suppression. It requires a primary input *d* (containing RFI) and a reference input *x*, which is obtained by delaying the primary input for some time-delay Δ. The adaptive linear combiner weighs and sums a set of input signals to form an adaptive output *y*. This output is an estimate of the RFI. The error signal *e*, which is the desired cleaned radar signal, is obtained by subtracting the RFI estimate *y* from the primary input *d*. The LMS adaptive algorithm minimises the mean-square error *e* by recursively altering the weight vector $\mathbf{W}$ at each sampling instant according to the Widrow-Hoff algorithm [11], yielding

$$\mathbf{W}_{j+1} = \mathbf{W}_j + 2\mu e(j)\,\mathbf{X}_j^* \tag{1}$$

where $\mathbf{X}_j^*$ is the complex conjugate of the reference signal vector at time *j*, *e(j)* is the error signal at time *j*, and μ is a constant convergence factor controlling stability and rate of adaptation.

RFI TRANSFER FUNCTION

The equivalent transfer function *H(ω)* of the LMS adaptive filter may be obtained once the filter tap weights have converged and are kept constant, making it unnecessary to feed the error signal *e* back into the adaptive filter. Fig. 2 shows the transfer function block diagram of the LMS adaptive filter with the weights kept constant. In the frequency domain, the output *E(ω)* is given by

$$E(\omega) = D(\omega) - Y(\omega) = D(\omega)\left[1 - F(\omega)G(\omega)\right]. \tag{2}$$

Therefore the equivalent transfer function *H(ω)* of the RFI suppression stage is given by

$$H(\omega) = \frac{E(\omega)}{D(\omega)} = 1 - F(\omega)G(\omega) \tag{3}$$

where *G(ω)* is the transfer function of the time-delay Δ, given by

$$G(\omega) = e^{-j\omega\Delta} \tag{4}$$

and *F(ω)* is the Fourier Transform of the *time-reversed* weight vector $\mathbf{W}$. Since we are dealing with digitised data, $\mathbf{W}$ must be zero-padded to the same length as the range compression transfer function described below.

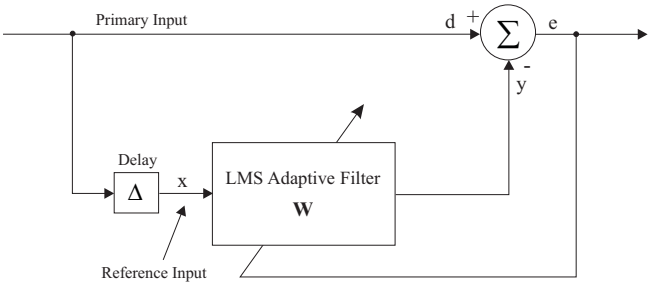

Fig. 1. *RFI suppression using an LMS adaptive filter.*

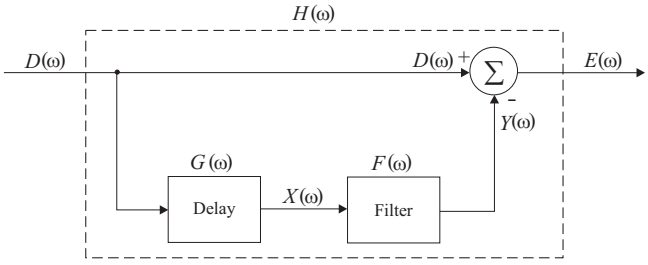

Fig. 2. *Block diagram of LMS adaptive filter with tap weights kept constant.*

INTEGRATION WITH RANGE-DOPPLER ALGORITHM

Range compression in the frequency domain is accomplished by multiplying the received signal with a matched filter $M(\omega)$, which is typically the complex conjugate of the transmitted pulse spectrum. The combined transfer function $T(\omega)$, which will simultaneously suppress RFI and perform range compression on the raw SAR image, is thus given by

$$T(\omega) = H(\omega)M(\omega). \tag{5}$$

SIDELOBE REDUCTION

Any interference suppressing filter will corrupt the desired signal with sidelobes. Abend and McCorkle [4] have described a sidelobe reducing procedure that has some similarities to the sidelobe reduction procedure presented in this paper. Fig. 3 shows a graphical illustration of the technique. In Fig. 3(a), the RFI contaminated signal passes through the LMS adaptive filter $H(\omega)$, yielding a signal free from RFI, but with introduced sidelobes. It is assumed that the RFI suppression is done perfectly, i.e. that there is no RFI present in the filtered output. In Fig. 3(b), the output from (a) is subtracted from the unfiltered signal, the result of which is again passed through the LMS adaptive filter, yielding a cleaned signal, which contains only the (negative) sidelobe. It is assumed that the sidelobe embedded in the RFI is already so small, that the output of the LMS adaptive filter does not contain any sidelobes of the sidelobe. Adding together the results of (a) and (b) yields the result shown in Fig. 3(c), which is just the cleaned signal without any sidelobes. The complete sidelobe reduction procedure is illustrated in block diagram form in Fig. 4. It can be shown that the overall transfer function is

$$H'(\omega) = \frac{E'(\omega)}{D(\omega)} = H(\omega)\left[2 - H(\omega)\right]. \tag{6}$$

The above assumption, namely, that the "sidelobes of the sidelobe" are negligible, is not always valid. The same procedure that was described above to suppress the original sidelobe can be used to suppress the "sidelobe of the sidelobe". The overall transfer function of this so-called "second-order" sidelobe reduction procedure is

$$H'_{2nd}(\omega) = H(\omega)\left[3 - 3H(\omega) + H(\omega)^2\right] \tag{7}$$

and the overall transfer function of the "k^{th}-order" sidelobe reduction procedure is [12]

$$H'_{k\,th}(\omega) = H(\omega)\sum_{n=0}^{k}\left[(-1)^n\ {}^{k+1}c_{n+1}\ H(\omega)^n\right] \quad \text{where} \quad {}^{a}c_b = \frac{a!}{(a-b)!\,b!} \tag{8}$$

The matched filter $M(\omega)$ in (5) will now be multiplied with $H'(\omega)$ instead of $H(\omega)$, thus incorporating the sidelobe reduction procedure, leading to a very efficient implementation. An example of a cleaned image is shown in Fig. 5.

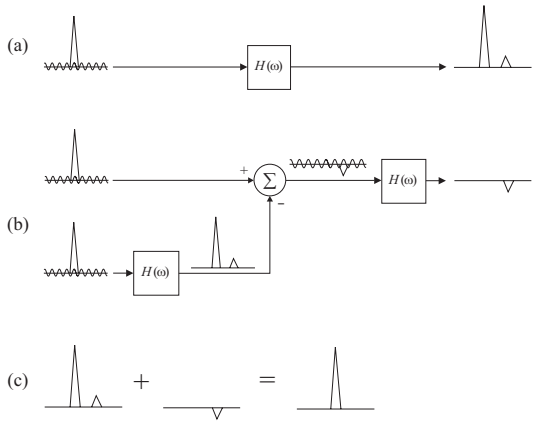

Fig. 3. Graphical illustration of sidelobe reduction procedure. The large triangle symbolises the wanted compressed target, the small triangle the unwanted sidelobe and the sinusoidal waveform the unwanted RFI interference.

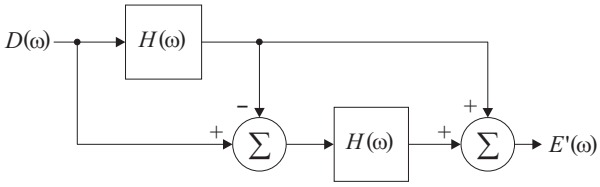

Fig. 4. Block diagram of sidelobe reduction procedure, where $H(\omega)$ is the transfer function of the LMS adaptive filter.

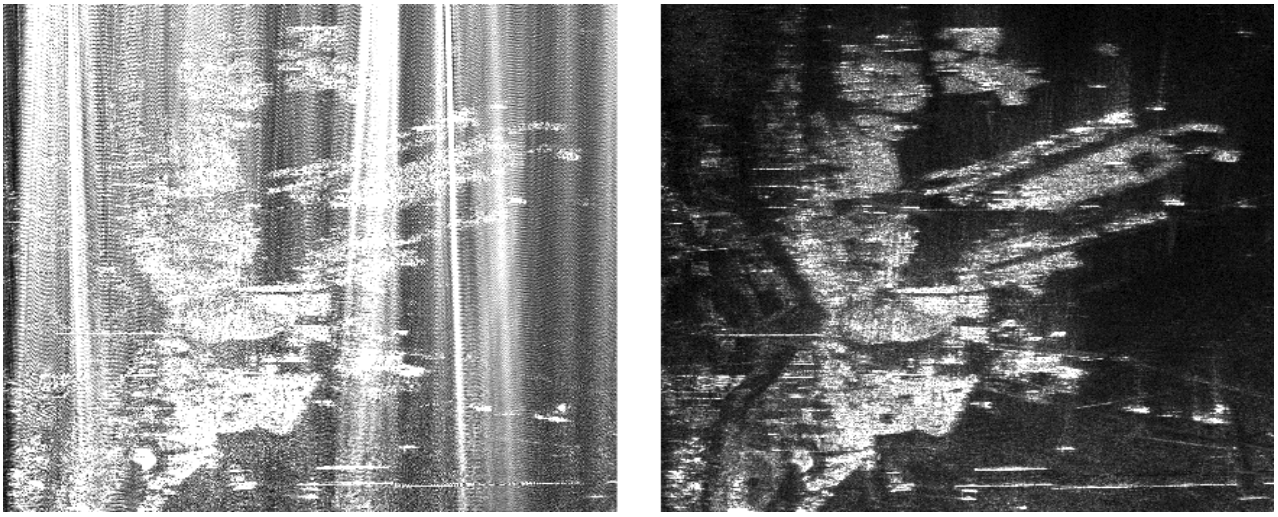

Fig. 5. *SASAR VHF-band image in South Africa, contaminated with RFI (left) and cleaned with the LMS adaptive filter (right). The flight path is along the horizontal axis, with near range towards the bottom of the image.*

CONCLUSIONS

This paper has described how the equivalent transfer function of the LMS adaptive filter, which is used to suppress RFI in SAR images, can be combined with the range compression transfer function of the range/Doppler SAR processor. This paper has also described a sidelobe reduction procedure, whose equivalent transfer function can be written in terms of the transfer function of the LMS adaptive filter. Thus a combined transfer function can be obtained, which implements RFI suppression, sidelobe reduction and range compression simultaneously, leading to a very efficient procedure. Our experience with P-Band and VHF-Band SAR data has shown that, once the tap weights of the adaptive filter have converged, the same set of tap weights (and therefore the same equivalent RFI transfer function) may effectively be used for up to a few hundred range lines.

REFERENCES

[1] M.R. Inggs, "The SASAR VHF Sensor," *Proc. European Conference on Synthetic Aperture Radar, EUSAR'96*, Königswinter, Germany, pp. 317–320, March 1996.

[2] P.A. Fridman and W.A. Baan, "RFI mitigation methods in radio astronomy," *Astronomy & Astrophysics*, 378, pp. 327–344, 2001.

[3] R. Ambrosini and V. Gobetti, "RFI Selection Criteria for New Radiotelescopes," *17th int. Wroclaw Symposium and Exhibition on Electromagnetic Compatibility, EMC 2004*, 29 June – 1 July 2004.

[4] K. Abend and J. McCorkle, "Radio and TV interference extraction for ultra-wideband radar," in *Algorithms for Synthetic Aperture Radar Imagery II*, (D.A. Giglio, ed.), SPIE, Orlando, FL, vol. 2487, pp. 119–129, April 1995.

[5] M. Braunstein, J. Ralston and D. Sparrow, "Signal processing approaches to radio frequency interference (RFI) suppression," in *Algorithms for Synthetic Aperture Radar Imagery*, (D.A. Giglio, ed.), SPIE, Orlando, FL, vol. 2230, pp. 190–208, April 1994.

[6] S. Buckreuss and R. Horn, "E-SAR P-Band SAR Subsystem Design and RF-Interference Suppression," *Proc. IEEE Geoscience Remote Sensing Symp., IGARSS'98*, Seattle, Washington, vol. 1, pp. 466–468, July 1998.

[7] T. Koutsoudis and L. Lovas, "RF Interference Suppression in Ultra Wideband Radar Receivers," in *Algorithms for Synthetic Aperture Radar Imagery II*, (D.A. Giglio, ed.), SPIE, Orlando, FL, vol. 2487, pp. 107–118, April 1995.

[8] T. Miller, J. McCorkle and L. Potter, "Near-least-squares radio frequency interference suppression," in *Algorithms for Synthetic Aperture Radar Imagery II*, (D.A. Giglio, ed.), SPIE, Orlando, FL, vol. 2487, pp. 72–83, April 1995.

[9] C.T.C. Le, S. Hensley and E. Chapin, "Removal of RFI in Wideband Radars," *Proc. IEEE Geoscience Remote Sensing Symp., IGARSS'98*, Seattle, Washington, vol. 4, pp. 2032–2034, July 1998.

[10] J. Li and P. Stoica, "Adaptive Filtering Approach to Spectral Estimation and SAR Imaging," in *Algorithms for Synthetic Aperture Radar Imagery II*, (D.A. Giglio, ed.), SPIE, Orlando, FL, vol. 2487, pp. 153–164, April 1995.

[11] B. Widrow, J.R. Glover, Jr., J.M. McCool, J. Kaunitz, C.S. Williams, R.H. Hearn, J.R. Zeidler, E. Dong, Jr., and R.C. Goodlin, "Adaptive Noise Cancelling: Principles and Applications," *Proc. IEEE*, vol. 63, no. 12, pp. 1692–1716, December 1975.

[12] Discussion with G. Tattersfield, University of Cape Town, South Africa, 1999.